Modeling the hydrological effects of climate and land use/cover changes in Chinese lowland polder using an improved WALRUS model

Renhua Yan, Junfeng Gao and Lingling Li

ABSTRACT

Hydrological processes in lowland polders, especially those for paddy rice planting, are affected by complicated factors. The improved Wageningen Lowland Runoff Simulator (WALRUS) model incorporates an irrigation and drainage scheme, and a new stage–discharge relationship to account for hydrological processes in multi-land-use polder with paddy fields and pumping stations. Here, this model was applied to assess how climate and land use changes affected the runoff of a Chinese polder in Poyang Lake basin in the past two decades. Simulated results showed that the runoff in the autumn–winter transition and midsummer months increased significantly, whereas those in the other months decreased slightly during the period of 1996–2005, primarily affected by climate change. For the period of 2006–2014, the runoff in the autumn–winter transition and midsummer increased, while that in the other months declined, affected by both climate and land use/cover changes. The land use/cover change resulting from the conversion of rice–wheat rotation to dominantly double-rice cropping and the expansion of residential area, increased the runoff during this period by demanding more irrigation water from the outside basin.

Key words | agricultural polder, climate change, improved WALRUS model, land use/cover change, modeling, runoff

Renhua Yan
Junfeng Gao (corresponding author)
Lingling Li
Key Laboratory of Watershed Geographic Sciences,
Nanjing Institute of Geography and Limnology,
Chinese Academy of Sciences,
73 East Beijing Road,
Nanjing 210008,
China
E-mail: *gaojunf@niglas.ac.cn*

Renhua Yan
School of Geographical Sciences,
Southwest University,
Chongqing 400715,
China

Renhua Yan
Lingling Li
University of Chinese Academy of Sciences,
Beijing 100049,
China

INTRODUCTION

Lowland polders are abundant in floodplains, particularly in the river deltas and lakeside zones of subtropical monsoon zones (Jiang *et al.* 2007; Zhao *et al.* 2010; Kovar *et al.* 2014). For example, the polders cover an area of 5,540 km^2 in Poyang Lake basin (Chen 1987), which is the largest freshwater lake in China. In the Taihu basin, East China, polders comprise approximately 30% of the total basin area (Yan *et al.* 2015). Land use/cover change and climate change are two of the most important factors that significantly impact the global hydrological processes. Previous studies have found that the changes in the annual and seasonal hydrologic components, including streamflow (Neupane & Kumar 2015; Yan *et al.* 2016a), precipitation (Júnior *et al.* 2015), evapotranspiration (Pavanelli & Capra 2014), temperature (Syvitski *et al.* 2009), and seepage (Immerzeel *et al.* 2009) are closely related to climate and land use/cover changes. These changes exacerbate catchment damage from extreme weather events (e.g. droughts and floods). The low elevation and flat terrain of lowland polders, as well as intensified human activities, have made lowland polders more vulnerable to the effects of droughts and flooding linked with both changes (Brauer *et al.* 2014a). Additionally, the hydrological response of polders to the climate and land use/cover changes will also have a direct effect on the transformation and delivery of pollutants into the downstream rivers,

doi: 10.2166/nh.2016.204

consequently affecting lake water quality because water flow is a carrier of agricultural pollutants. Therefore, better study of the influences of land use/cover and climate changes on polder hydrology is crucial to mitigating natural disasters, reducing eutrophication, and advancing water resources management that directly affect the daily life of a great number of local residents.

Some previous studies have analyzed how climate change and land use/cover change affect the timing and magnitude of discharge, surface water level, seepage, and flood events in west European polders, such as those in western Netherlands and northeastern Germany (Immerzeel *et al.* 2009; Bouwer *et al.* 2010; Hellmann & Vermaat 2012). However, very few studies focused on polders in Asian monsoon zones. Compared to the west European polders, polders in Asian monsoon zones have distinct climatic conditions (monsoon climate), cropping patterns (dominated by paddy rice), and water management regimes (submerged irrigation and pumping-induced drainage). These features may cause polders to exhibit different responses to climate change and land use/cover change. Accordingly, assessing the effects of climate and land use/cover changes on the polders in Asian monsoon zones may contribute to a more comprehensive understanding of their hydrological effects on the polders in different climates and areas. Nevertheless, most Asian polders are poorly gauged, and do not have complete historical runoff datasets.

Hydrological models have been widely used by hydrologists as a tool for analyzing the relationship between land use/cover change, climate change and hydrological processes, such as Soil and Water Assessment Tool (SWAT) (Guse *et al.* 2015; Mehdi *et al.* 2015; Awan *et al.* 2016), Water Flow Model for Lake Catchment (Li *et al.* 2013), Back-Propagation Neural Network (Li *et al.* 2015), Hydrological Simulation Program Fortran (Estes *et al.* 2015), Precipitation-Runoff Modeling System (Legesse *et al.* 2003), GR4J (Folton *et al.* 2015), and Xin'anjiang models (Yan *et al.* 2016a). The simulated results from the calibrated models can compensate for the scarcity and discontinuity of hydrological datasets. However, these existing models have been designed mainly for freely draining catchments with sloping surfaces rather than for flat polders with shallow groundwater and complicated water management operations, because some polder-specific hydrological characteristics (e.g. capillary rise and effect of surface water on groundwater table) are not explicitly considered. Faced with these problems, Brauer *et al.* (2014b) recently proposed a lumped rainfall–runoff model called the Wageningen Lowland Runoff Simulator (WALRUS) to account for three essential processes in lowland polders: groundwater – surface water feedback, saturated and unsaturated zone coupling, and wetness-dependent flow routes. Based on this model, an improved WALRUS model was developed for application in multi-land-use polder with paddy fields and pumping stations in Asian polders. The improved WALRUS model describes the runoff from different sources (e.g. paddy fields, residential areas, dry farmlands, and water areas) and introduces an irrigation and drainage scheme to control water management in paddy fields.

In this study, the proposed model is applied to quantify and discriminate the hydrological consequences of climate and land use/cover changes in the large polder of Poyang Lake basin in East China in the past few decades. The objectives of this study were to (1) simulate the response of the seasonal and annual runoff to climate change alone and land use/cover change alone, respectively, and (2) compare the sensitivity of runoff to climate variability and to land use/cover change. This study can be used to understand the present situation and provide references for adaptive water management decisions that affect the sustainability of social–ecological systems in polder catchments.

STUDY AREA AND DATA

Study area

The Jiangxiang Polder (28°43′–28° 54′N, 115°56′–116°15′E) located in the central part of Poyang Lake basin drains a catchment of 149.9 km^2 (Figure 1). This polder is enclosed between the middle and south branches of the Ganjiang River, which flows south to north and eventually drains into Poyang Lake. The water areas, which are composed of ditches and ponds, have extensive distribution in the catchment, and their water levels are controlled by pumping stations that drain surplus water toward the Ganjiang River during flood periods. Six large pumping stations generalized from dozens of realistic pumps exist along the dike. These pumping stations are used not only

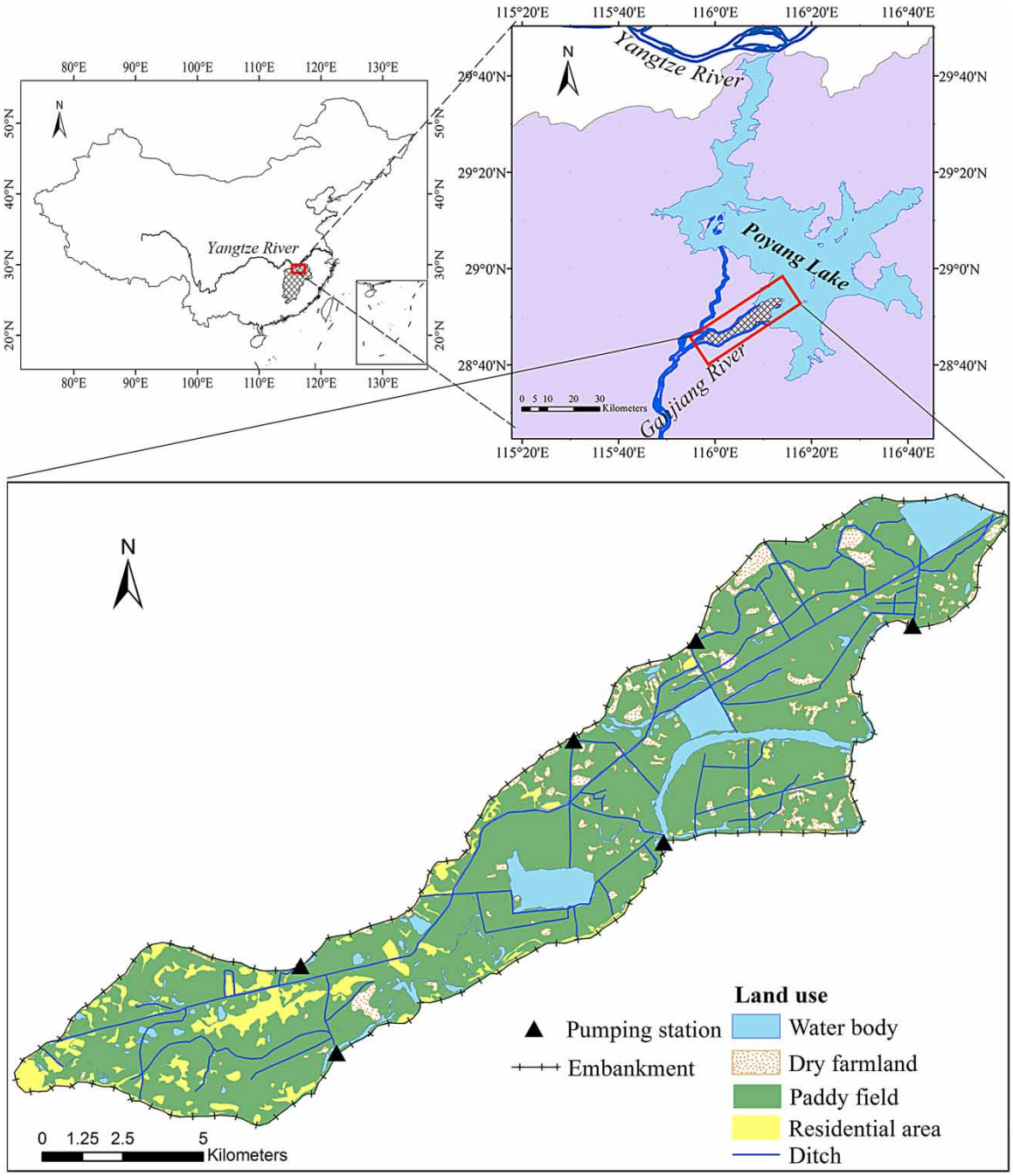

Figure 1 | Location of Jiangxiang polder and its land use types (in 2010). Please refer to the online version of this paper to see this figure in color: http://dx.doi.org/10.2166/nh.2016.204.

for draining floodwater, but also for pumping irrigation water for paddy rice growth.

Table 1 provides a summary of the land use classifications at different times (1990, 2000, and 2010). The catchment, as shown in Table 1, is dominated mainly by paddy fields with rice–wheat rotation (more than 70% of the catchment). During the rice growth period, submerged irrigation is necessary to maintain continuous inundation in the paddy fields. In general, irrigation water is pumped from outside the catchment, that is, from the Ganjiang

Table 1 | Percent cover of land use types in the Jiangxiang polder derived from remote sensing data of 1990, 2000, and 2010

Land use type	1990 (%)	2000 (%)	2010 (%)
Paddy field	79.7	78.6	74.8
Dry farmland	6.1	6.2	7.2
Water body	11.0	11.1	11.3
Residential area	3.3	4.1	6.7

River. Other minor land uses are dry farmland, water area, and residential area. Although significant changes in land use percentages have not been found in the last few decades, the conversion from rice–wheat rotation system to double-rice cropping system in the paddy fields since 2006 has drastically altered the agricultural landscape, which could have also affected the hydrological cycle of the study area. The dominant soil texture is silt loam.

The region is characterized by East Asian monsoon climate with an annual mean temperature of 17.6 °C and an average potential evaporation of 1,050 mm. The average annual precipitation is 1,612 mm (1980–2014), with 69% occurring during the rainy period (April–September).

Data

The basic dataset required for the improved WALRUS model includes weather, land use, soil, and pump discharge. For this study, land use data were interpreted from Landsat Thematic Mapper images with 30×30 m resolution acquired in 1990, 2000, and 2010. Soil type data were obtained from the field investigations. The weather variables used were daily precipitation (mm), maximum and minimum temperature (°C), and potential evapotranspiration (mm). Most of the weather variables were derived from the national weather station at Nanchang (No. 58606), about 28 km southwest of the center of the study area. Reference evapotranspiration was calculated with the Hargreaves equation (Hargreaves & Samani 1985), based on the daily maximum and minimum temperatures. Thereafter, the calculated reference evapotranspiration was multiplied by different crop coefficients to estimate the potential evapotranspiration of paddy field and dry farmland, respectively (Gao 2004). The surface water evaporation was assumed to be equal to the reference evapotranspiration of a well-watered soil (Brauer *et al.* 2014b). The coefficient of determination (R^2) between the calculated daily evapotranspiration of surface water and the observed pan evaporation was 0.39 ($p = 0.000$) for the period of 2006–2008, which justified the use of the Hargreaves method for the study area. The weather data covered the period from 1986 to 2014. To test the model accuracy, the observed monthly runoff from 2006 to 2008 taken from the study of Luo *et al.* (2013) and Su *et al.* (2013) were used.

METHODOLOGY

Model description

The improved WALRUS model was developed in R and conceptually based on the WALRUS model. The user can choose at which times output should be produced (e.g. hourly, daily or non-equidistant). Internally, the computation time step is reduced if necessary (e.g. too much rain or water level variation). This variable time step approach increases stability. The model consists of four compartments: dry farmland, paddy field, water area (surface water), and residential area.

The dry farmland and paddy field include two reservoirs: a quickflow reservoir and a soil reservoir (coupled vadose–groundwater reservoir). Precipitation is the most important water source. At the field surface, precipitation is divided by the soil wetness index (W) into a portion that percolates to the soil matrix (P_V) and another portion that is directly led to the surface water through a quick flow path (P_Q). Water is depleted by evapotranspiration from the vadose zone (ET_V). The dryness of the vadose zone is expressed by a state variable of storage deficit (d_V), that denotes the amount of water required to saturate the soil profile and determines the evapotranspiration reduction (β) and wetness index (W). Taking dry farmland as an example, the relation between evapotranspiration reduction (β_2) and storage deficit (d_{V2}) is specified as follows:

$$\beta 2 = \frac{1}{2} \cdot \frac{1 - \exp[\zeta_1 (d_{V2} - \zeta_2)]}{1 + \exp[\zeta_1 (d_{V2} - \zeta_2)]} + \frac{1}{2}$$

Thus, the evapotranspiration of the vadose zone (ET_{V2}) is calculated as follows:

$$ET_{V2} = ET_{pot2} \cdot \beta 2 \cdot a_{G2}$$

where ET_{pot2} denotes the potential evapotranspiration of the dry farmland, a_{G2} the dry farmland area fraction, and ζ_1 and ζ_2 the two parameters. A detailed description of these variables and parameters is listed in Table A1 (available with the online version of this paper) and can also be referred to Brauer *et al.* (2014b).

The groundwater table (d_G) has a dynamic response to change in storage deficit and controls in combination with the surface water level (hs), groundwater drainage or infiltration of surface water (f_{GS}). Groundwater drainage flux (f_{GS}) can be either positive or negative depending on the differences in water level between the surface water (hs) and groundwater (d_G), that considers the groundwater–surface water interaction and infiltration of surface water into the soil reservoir with higher surface water level. All water that does not pass through the soil matrix is delivered to the surface water through a quickflow route (f_{QS}), which represents overland flow, local ponding, and macropore flow. Seepage (f_{XG}) is also taken into account in the model and represents the water being added to or subtracted from the soil reservoir. The aforementioned processes are shared by the dry farmland and paddy field. In addition, a water management scheme with three critical water depths (lower limit of appropriate depth ($h_{Q,min1}$), upper limit of appropriate depth ($h_{Q,max1}$), and maximum submergence-tolerant water level ($h_{Q,flood1}$) for rice growth) (Guo 1997; Xie & Cui 2011) is incorporated into the model to control the irrigation and drainage in the paddy field. The water depth in the field surface (i.e. level of quickflow reservoir of paddy field h_{Q1}) should be kept within the range between the $h_{Q,min1}$ and $h_{Q,max1}$ to provide preferable moisture condition for rice growth. In case the water depth in the field surface (h_{Q1}) drops below $h_{Q,min1}$, denoting that moisture might threaten rice growth, the irrigation operation is required to execute until the depth reaches $h_{Q,max1}$. In contrast, with extreme rainfall event occurring, in case the water depth exceeds $h_{Q,flood1}$, field drainage operation needs to be implemented. In other words, the quickflow in the paddy field (f_{QS}) will be activated only if the depth of the quickflow reservoir exceeds $h_{Q,flood1}$. We should note that the three critical depths are changeable over the cropping regime and growth stages of paddy rice (Tables 2 and 3).

For the residential area, which is considered as an impervious area, precipitation is assumed not to percolate into the soil matrix but directly routes into the adjoining

Table 2 | Three critical water depths (mm) of paddy field at different growth stages of single cropping of rice in Poyang Lake basin

		Tillering						
Growth stage	**Steeping**	**Early**	**Midterm**	**Late**	**Booting**	**Heading**	**Milking**	**Ripening**
Date	6/21–6/30	7/1–7/20	7/21–8/3	8/4–8/10	8/11–9/3	9/4–9/10	9/11–9/25	9/26–10/10
$h_{Q,min1}$-$h_{Q,max1}$-$h_{Q,flood1}$	20-40-80	20-30-70	20-30-80	0-0-0	20-50-90	10-30-50	10-20-60	0-0-0

After Gao (2004), Cheng *et al.* (2006) and Cai *et al.* (2014).

Table 3 | Three critical water depths (mm) of paddy field at different growth stages of double cropping of rice (early rice and late rice) in Poyang Lake basin

			Tillering					
Growth stage		**Steeping**	**Early**	**Late**	**Booting**	**Heading**	**Milking**	**Ripening**
Date	Early rice	4/21-4/30	5/1–5/23	5/24–5/31	6/1–6/23	6/24–6/30	7/1–7/15	7/16–7/20
	Late rice	7/21–7/30	7/31–8/22	8/23–8/30	8/31–9/22	9/23–9/29	9/30–10/14	10/15–10/30
$h_{Q,min1}$-$h_{Q,max1}$-$h_{Q,flood1}$		20-40-80	20-30-70	0-0-0	20-50-90	10-30-50	10-20-60	0-0-0

surface water within a short time. In the model, a runoff coefficient is used to calculate the drainage of the residential areas, which represents water loss from evapotranspiration and surface depression storage.

For the water area, water inputs include precipitation (P_s), the drainages of paddy field ($f_{QS1}+f_{GS1}$) and dry farmland ($f_{QS2}+f_{GS2}$), and residential area (f_{rS}). Water consumption terms consist of evapotranspiration (ET_s) and catchment runoff (Q). Catchment runoff (Q) is calculated as a function of surface water level (h_S) and threshold water level to start pumping (hS^{start}_{pump}):

$$Q = \begin{cases} 0 & h_S \le hS^{start}_{pump} \\ Q_{pumping} & h_S > hS^{start}_{pump} \end{cases}$$

where Q_{pump} is obtained from converting the pump capacity (m^3/s) to mm/h by dividing the polder area.

The modeling approach is shown schematically in Figure 2. Table A1 displays the model equations, variables, and parameters.

Model calibration and validation

There are four types of model parameters including the wetness index parameter (c_{w1} and c_{w2}), vadose zone relaxation time (c_{v1} and c_{v2}), groundwater reservoir constant (c_{G1}, c_{G2}, and c_{G3}), and quickflow reservoir constant (c_{Q1} and c_{Q2}), that need to be optimized to represent the catchment-specific characteristics. Based on the field investigation, the threshold water level to start pumping (hS^{start}_{pump}) and ditch depth (c_D) in the study area were estimated to be 1,000 and 1,500 mm, respectively. The three critical water depths for the paddy field irrigation and drainage scheme are listed in Tables 2 and 3. According to the table of parameters taken from the results of Clapp & Hornberger (1978) and Brauer et al. (2014b) used in the model, the parameters values of soil moisture profile including pore size distribution parameter b, air entry pressure ϕ_{ae}, and soil saturated moisture content θ_S were identified based on soil type.

For the calibration and validation, the total runoff aggregated from six large pumping stations was employed to test the developed model. In general, the Chinese polders are poorly gauged because of the absence of fixed hydrological measuring stations to collect long-term and continuous monitoring records. Therefore, only 3 years' runoff data at a monthly time scale (deduced from the pumping capacity and recorded operational time) were available to test the accuracy of the model in this study. The first 2 years (from January 2006 to December 2007) were used for calibration and the subsequent year (from January 2008 to December

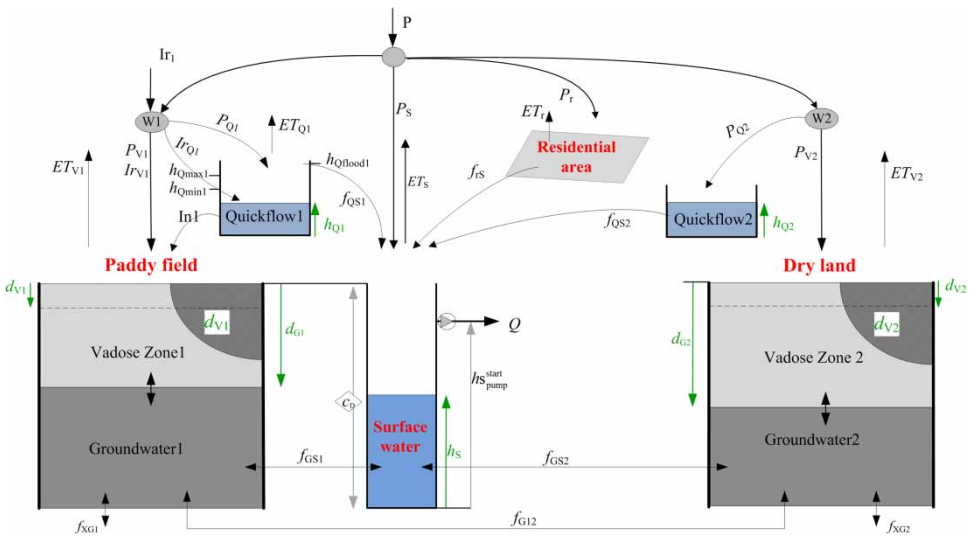

Figure 2 | Schematic representation of the improved WALRUS model. Black arrows represent water fluxes and cyan arrows stand for the reservoir states. Please refer to the online version of this paper to see this figure in color: http://dx.doi.org/10.2166/nh.2016.204.

2008) for validation. This study used the model to simulate the runoff at a daily scale. Then the simulated daily results were aggregated into monthly values for validating the model by comparing the modeled runoff with the measured values. The two commonly used indicators, namely, the Nash–Sutcliffe coefficient (E_{NS}) and coefficient of determination (R^2), were applied to evaluate model performance. The main input data for the calibration and validation are shown in Figure 3.

Model scenarios and simulation

According to the study of Tian (2012), the annual hydro-meteorology variables of the Poyang Lake basin (Jiangxiang polder is subordinate to this basin), especially temperature and precipitation, tended to increase since the 1990s and their abrupt change points were identified around 1996 by using the non-parametric Mann–Kendall trend test (Mann 1945; Kendall 1975) and Mann–Kendall–Sneyers method

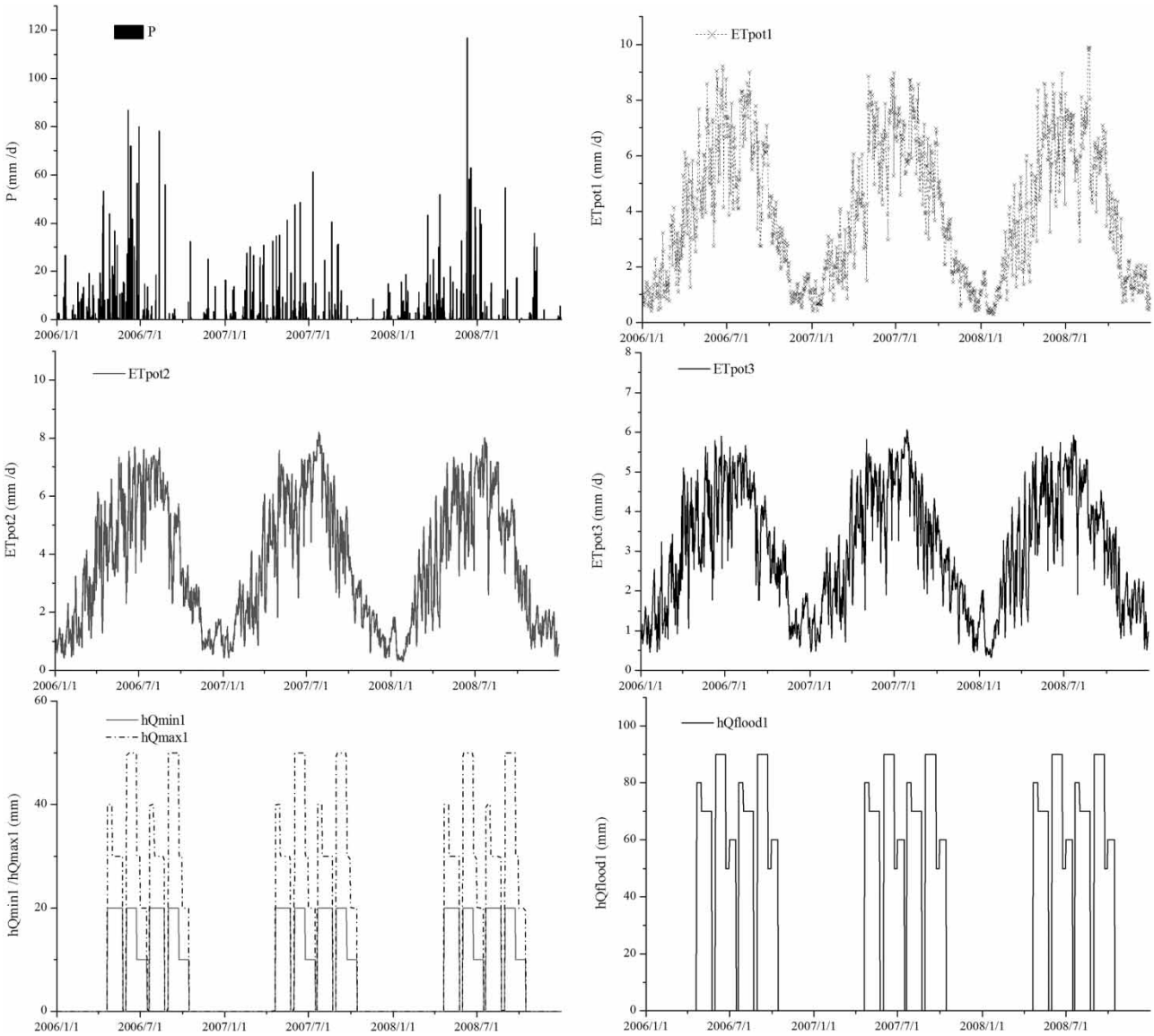

Figure 3 | Main input data of the model for the calibration and validation.

(Sneyers 1975) to detect the hydro-meteorology changes over the last 50 years. Furthermore, as a result of China's new agriculture policy for tax relief and increased farm subsidies since 2004 and the advances in agricultural technology, paddy fields have begun to be dominated by double-rice cropping system for higher profit since 2006 (Li *et al.* 2014). This major land use/cover change may have great impact on the polder runoff. Therefore, based upon the aforementioned analyses, a fixed time interval, and the data availability, the period of 1986–2014 was selected to analyze the hydrological effect of climate and land use/cover changes and was divided into three periods: 1986–1995 (baseline period), 1996–2005 (impact period), and 2006–2014 (impact period).

The improved WALRUS simulation of runoff was implemented for the three periods. In order to assess the hydrological impacts of historical land use/cover and climate changes, five scenarios (Table 4) were established and were modeled with the calibrated model as follows: Scenario 1, for which the climate data during the period 1986–1995 and the land use data from 1990 were utilized, was regarded as the conditions for the baseline period (1986–1995). In Scenario 2 and Scenario 3, the land use remained constant, while the climate data were altered for the periods of 1996–2005 and 2006–2014, respectively. The simulated results are the results of climate change alone for the latter two periods. Scenario 4, for which the land use data in 2000 and the climate data during the period of 1996–2005 were employed, was regarded as the situation for the period 1996–2005, while Scenario 5, for which the land use data from 2010 and the climate data during the period of 2006–2014 were employed, was used as the situation for the period 2006–2014. The simulated results are the combined results of climate and land use/cover changes. Therefore, there were five model runs for simulation of historical changes in polder runoff.

Table 4 | Summary of model scenarios

Scenario	Land use/cover	Climate
1	1990	1986–1995
2	1990	1996–2005
3	1990	2006–2014
4	2000	1996–2005
5	2010	2006–2014

According to Guo *et al.* (2014), the climate change effect ($\Delta Q_{\text{climate}}$) for the latter two periods (1996–2005 and 2006–2014) was quantified by comparing the modeled results under Scenario 2 ($Q_{Scenario2}$) and Scenario 3 ($Q_{Scenario3}$) with those under Scenario 1 ($Q_{Scenario1}$), respectively. The land use/cover change effect was also computed by comparing the simulated results under Scenario 4 ($Q_{Scenario4}$) and Scenario 5 ($Q_{Scenario5}$) with those under Scenario 2 ($Q_{Scenario2}$) and Scenario 3 ($Q_{Scenario3}$), respectively. The combined effect of land use/cover and climate changes (ΔQ) was also analyzed by comparing the simulated results under Scenario 4 ($Q_{Scenario4}$) and Scenario 5 ($Q_{Scenario5}$) with those under Scenario 1, respectively. Therefore, the relative effects of climate change (I_{climate}) and land use change (I_{lucc}) were quantified using the following equations:

$$I_{\text{climate}} = \frac{\Delta Q_{\text{climate}}}{\Delta Q} \times 100\% \quad (1)$$

$$I_{\text{lucc}} = \frac{\Delta Q_{\text{lucc}}}{\Delta Q} \times 100\% \quad (2)$$

$$\Delta Q_{climate} = Q_{Scenario2/3} - Q_{Scenario1} \quad (3)$$

$$\Delta Q_{lucc} = Q_{Scenario4/5} - Q_{Scenario2/3} \quad (4)$$

$$\Delta Q = Q_{Scenario4/5} - Q_{Scenario1} \quad (5)$$

RESULTS AND DISCUSSION

Calibration and validation

Most parameters values were preset by referring to the values reported for the Jianwei polder, Taihu basin, improved WALRUS application reported by Yan *et al.* (2016b), and then were calibrated with a trial-and-error method (Table 5). The calibration and validation results are graphically presented in Figures 4 and 5. Moreover, the daily simulated values are shown in Figure 6.

Table 5 | Summary of calibrated parameter values for the Jiangxiang polder

Parameter (unit)	c_{w1} (mm)	c_{w2} (mm)	c_{v1} (h)	c_{v2} (h)	c_{G1} ($\times 10^6$mm h)	c_{G2} ($\times 10^6$mm h)	c_{G3} ($\times 10^6$mm h)	c_{Q1} (h)	c_{Q2} (h)
Calibrated value	145	110	19	11	65	30	92	4	2

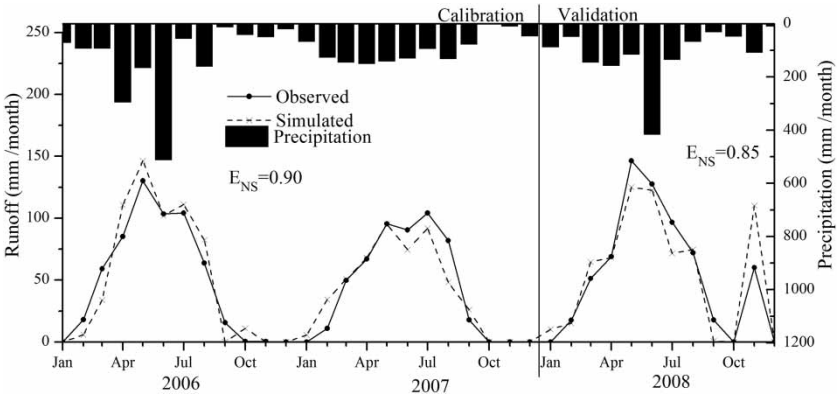

Figure 4 | Monthly simulated and observed runoff for the Jiangxiang polder in the calibration (2006–2007) and validation period (2008).

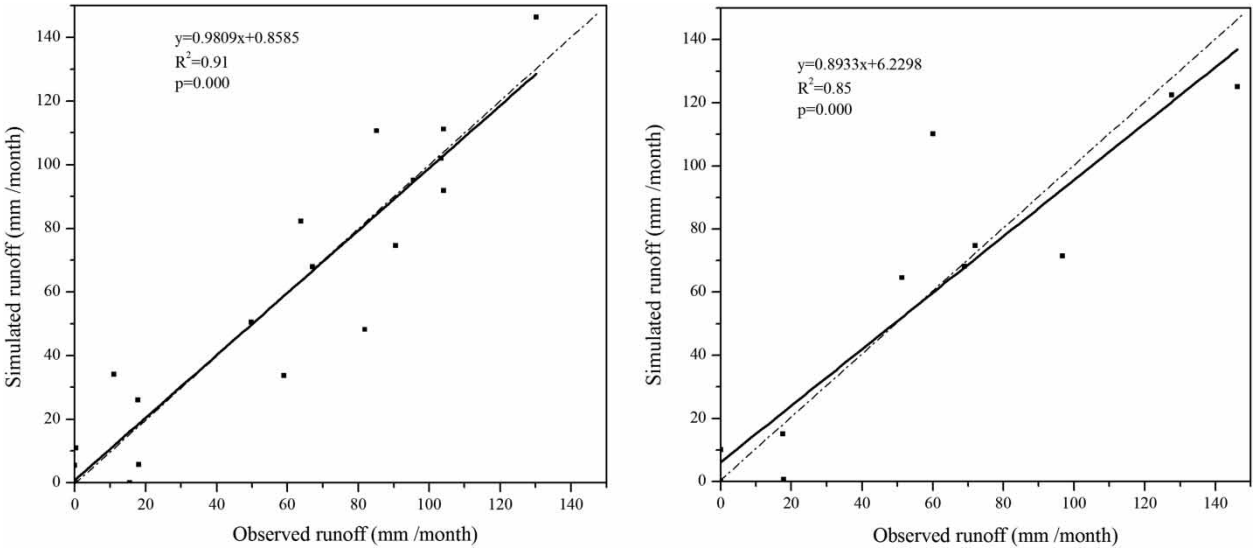

Figure 5 | Monthly simulated versus observed runoff relationship for the calibration (2006–2007) (left) and validation period (2008) (right).

The improved WALRUS model closely tracked the magnitudes and fluctuations of the monthly runoff for both periods. The Nash–Sutcliffe coefficient (E_{NS}) and coefficient of determination (R^2) were larger than 0.9 for the calibration period and larger than 0.8 for the validation period (Figures 4 and 5), and the scatter diagrams of the simulated and observed runoff values for the two periods were both distributed along the 1:1 fit line, with the slopes of the linear regression lines approaching 1. These results indicated that the calibrated model reasonably represented the hydrological processes in the current polder and provided accurate estimates of polder runoff.

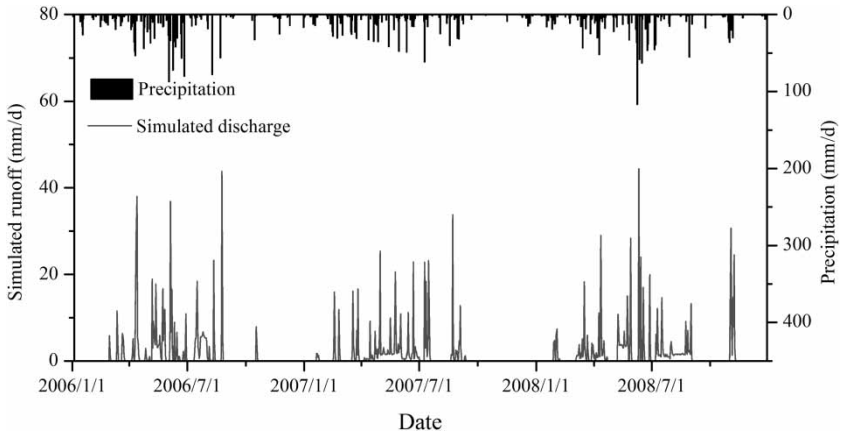

Figure 6 | Daily simulated runoff for the calibration and validation period.

Climate change impact

Figure 7 illustrates the comparison of the runoff value affected by climate change alone for the latter two periods (1996–2005 and 2006–2014) versus the runoff value in the baseline period (1986–1995). A large variation in the monthly runoff was found between the latter two periods and the baseline period, indicating that climate change had a considerable effect on the monthly runoff for the two latter periods. The runoff significantly increased for the autumn–winter transition (November–January) and midsummer (August) months. For example, the runoff for both periods increased by approximately 200% compared to that for the baseline period in December. Conversely, the runoff in the other months, including early spring and autumn, slightly decreased at a rate lower than 50%. This seasonal variation in the climate effect is the combined result of the changes in precipitation and temperature (Figure 8). In the autumn–winter transition and midsummer months, the precipitation in the latter two periods was much larger than those in the baseline period. Furthermore, the lower temperature contributed to the decrease in evapotranspiration relative to the baseline period. Hence, the expanded net rainfall caused an increase in the monthly runoff for the later two periods. In contrast, a decrease in monthly precipitation during the early spring and autumn was accompanied by an increased temperature, which in turn resulted in an increase in evapotranspiration from the baseline period. Thus, the runoff during early spring and autumn was reduced by the reduction in precipitation and increase in evapotranspiration. However, the effect of precipitation change on streamflow was larger than that of temperature in terms of the degree of similarity between the trends in

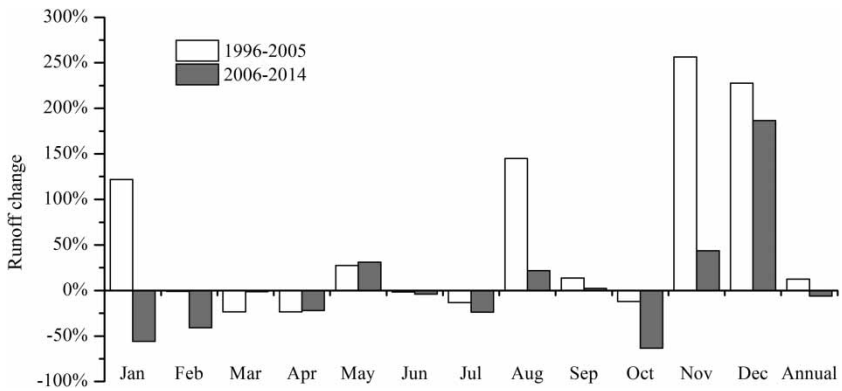

Figure 7 | Comparison of runoff affected by climate change alone for the latter two periods (1996–2005 and 2006–2014) versus the runoff in the baseline period.

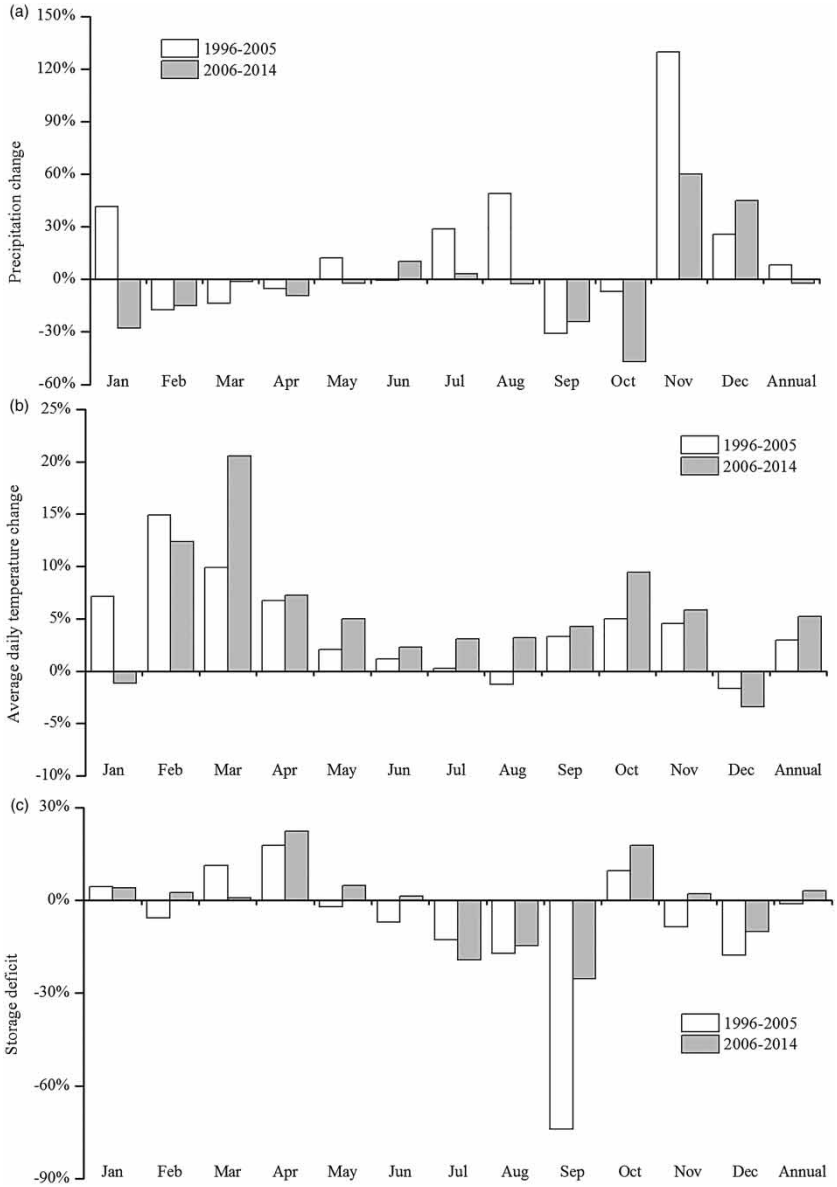

Figure 8 | Comparison of precipitation, temperature, and storage deficit between the baseline period and the latter two periods.

climate factors and runoff. That might also be proven by the correlation of runoff with climate factor changes, which implied that although the two climate factors were statistically significant as related to runoff, the runoff was more correlated with precipitation ($R = 0.706$, $p = 0.000$) than with the temperature ($R = -0.466$, $p = 0.022$) for both the periods. Moreover, it is remarkable that the precipitation increased during the early summer (June and July), whereas the runoff decreased. It might be attributable to the buffer capacity of the soil. Soil moisture was depleted more rapidly by evapotranspiration in the drier spring than in the baseline period (as evidenced by the increased storage deficit), which provided a buffer capacity for the increased early summer precipitation (Figure 8(c)). As a result, although the early summer period experienced high precipitation, little runoff occurred because the increased rainfall was stored in the soil to compensate for the excessive depletion of water in the previous

season, when the initial soil water content was lower than that in the baseline period.

While the climate effect from 1996 to 2005 was relatively greater than that from 2006 to 2014, the overall seasonal pattern of the change in the runoff between both periods was consistent, possibly because no considerable differences in the direction of precipitation and temperature changes were observed between the two periods.

In addition to the influence of climate change on the seasonal distribution of runoff, climate change also had a profound effect on the annual amount of runoff during the period of 1996–2005, notwithstanding that the impact was relatively smaller than that on the monthly values. The annual runoff for the period of 1996–2005 increased by 12.6% compared to the corresponding values in the baseline period, which was due to the 8.2% increase in annual precipitation. This finding is similar to that of a previous study on the upper reaches of the Ganjiang (Tian 2012), which found a 19.7% increase in the streamflow because of climate change for the same period by using historical hydro-climatic data and the SWAT model. This result can also be proven by historical meteorological statistics, which shows that the period of 1996–2005 was one of the wettest periods over the past five decades. During this period, two extreme flood events in 1998 and 1999 occurred in the Poyang Lake basin. Nevertheless, during the period of 2006–2014, the annual runoff remained similar to that in the baseline period, indicating that the climate change primarily affected the temporal variations of runoff for this period instead of the annual runoff.

Land use/cover change impact

Figure 9 shows the change in the runoff affected by land use change for the latter two periods (Scenarios 4 and 5) compared to the corresponding values for the 'constant' land use/cover change scenario (Scenarios 2 and 3). The runoff in the period of 1996–2005 was less affected by the land use/cover change, because there was almost no change in all the months and in the annual runoff for the same period.

However, during the period of 2006–2014, land use/cover change had a substantial effect on the monthly runoff. The runoff exhibited a considerable increase in all the months (except April and September), especially during the rice-growing period (from May to October) with a maximum increase of 88.1%. For instance, most monthly runoff during the rice-growth period increased by more than 30%. This result may be attributed to two reasons: the change in the cropping pattern of paddy field and increased residential area. Indeed, affected by China's new agriculture policy for tax relief and increased farm subsidies since 2004 and the advances in agricultural technology, paddy fields have begun to be dominated by double-rice cropping system for higher profit (Li *et al.* 2014). The conversion from prior rice–wheat rotation to double-rice cropping in the paddy field involves additional irrigation water derived from outside the basin to improve soil water conditions for rice growth. Annual data indicates that under the same climate condition, the average amount of irrigation water used by double-rice cropping was 572.9 mm/a as compared to rice–wheat rotation of

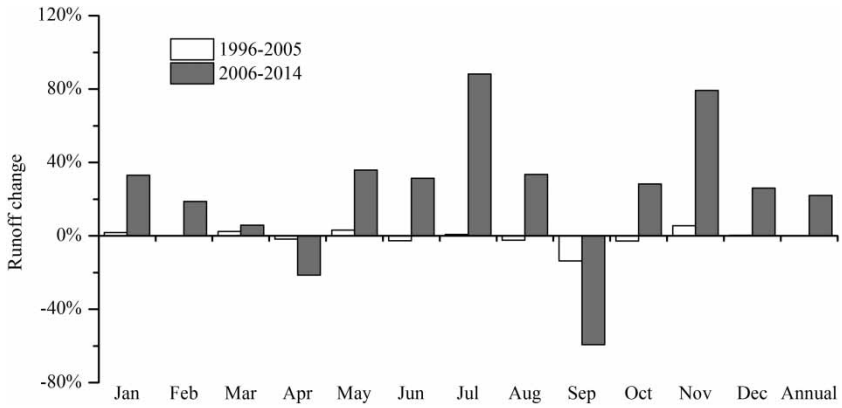

Figure 9 | Comparison of runoff affected by the land use/cover change versus the corresponding value for 'constant' land use/cover change scenario in the latter two periods.

397.9 mm/a. However, the actual evapotranspiration slightly increased by 34.4 mm/a compared to rice–wheat rotation (Figure 10). As a result, this difference in water balance, in turn, was sufficient to cause greater runoff for the double-rice cropping than that of rice–wheat rotation. Furthermore, with the expansion of residential area from 3.28% in 1990 to 6.69% in 2010, a reduction in plant transpiration and soil evaporation from the surface relative to the previously vegetated surface induced more rainfall routed directly into runoff. These factors ultimately increased the polder runoff.

Since most of the monthly runoff increased, the annual runoff also had a significant increase with a rate of 22.1% during the period of 2006–2014. Thus, land use/cover change affected both the temporal runoff distribution and the change in the annual amount of runoff from 2006 to 2014. This finding is contrary to the effect of climate change alone, which slightly reduced the annual runoff. Combined with the finding from the last section 'Climate change impact', it can be concluded that the runoff from 2006 to 2014 was sensitive to both land use change and climate change, while the runoff during the period of 1996–2005 was more affected by climate change than by land use/cover change.

Combination of both impacts

In order to evaluate the combined impact of climate and land use/cover changes, the comparison of the runoff during the latter two periods (Scenarios 4 and 5) and in the baseline period (Scenario 1) are depicted in Figure 11.

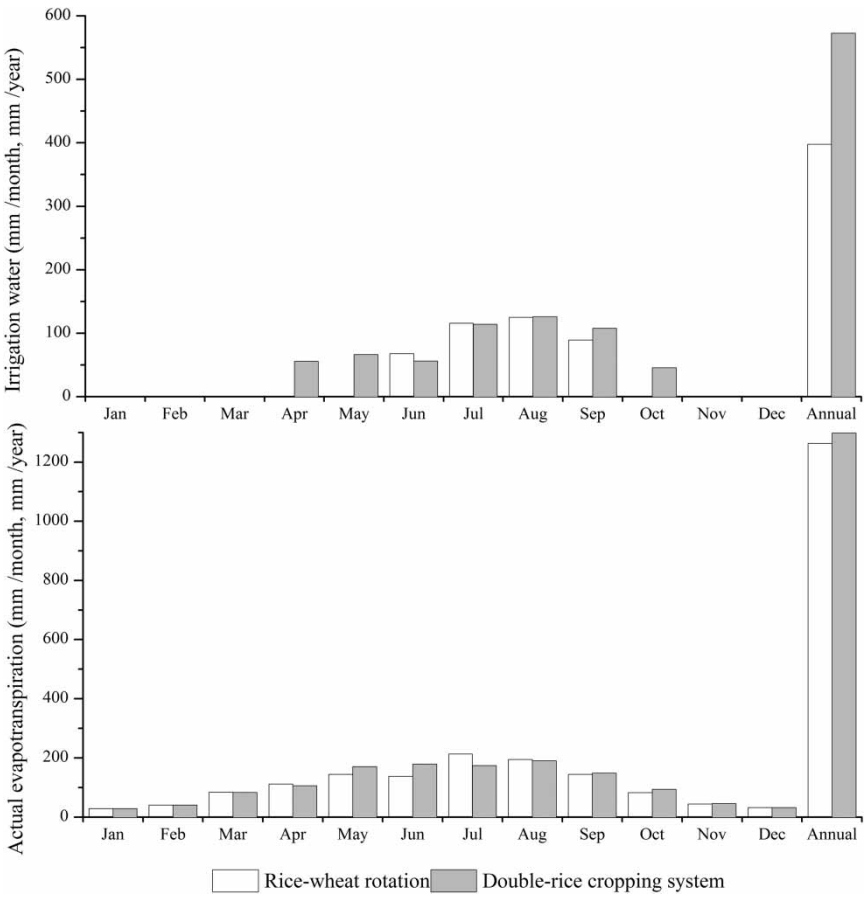

Figure 10 | Irrigation water and actual evapotranspiration for the rice–wheat rotation (top) and the double-rice cropping (bottom) under the same climate conditions (2006–2014) within the polder.

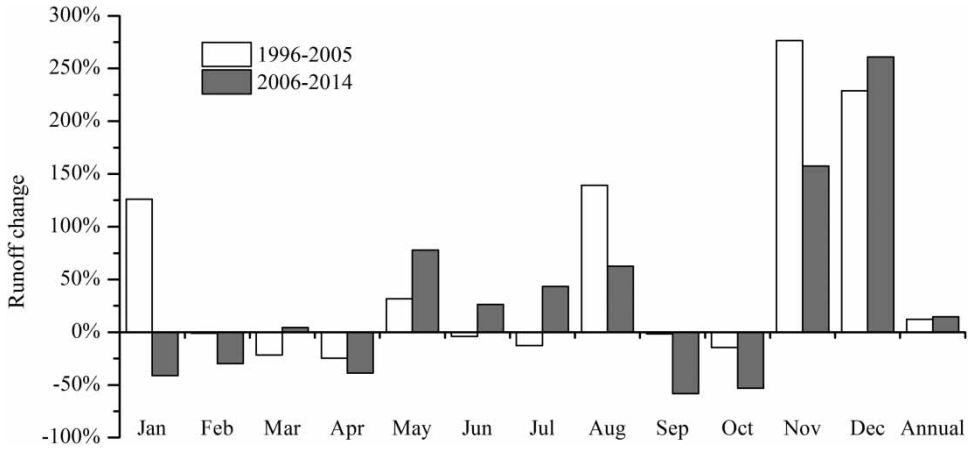

Figure 11 | Comparison of runoff affected by the combined effect of climate and land use/cover changes for the latter two periods versus the runoff in the baseline period.

As runoff was less affected by land use change, the runoff in the period of 1996–2005 affected by the concurrent impacts of climate and land use/cover changes was similar to that influenced by climate change alone. For this period, the runoff in the autumn–winter transition and midsummer months increased, whereas those in the early spring and autumn decreased. For the period of 2006–2014, as illustrated in the section 'Land use/cover change impact', climate and land use/cover change both had important influences on the runoff change. Consequently, in case the direction of the climate impact was consistent with that of the land use/cover change, the change in the runoff was enlarged when the climate and land use/cover changes occurred simultaneously. For instance, the runoff in the autumn–winter transition and midsummer months under both climate and land use/cover change conditions increased at a higher rate than those under the climate change condition alone during the period of 2006–2014. On the contrary, in case the directions of both effects are converse, the magnitude of the runoff change decreased when climate change together with land use/cover change occurred. For example, in October of the period 2006–2014, the decrease rate of runoff affected by both effects was reduced to 53.1%, which was lower than that affected by climate change alone (63.4%). The combined effect of climate and land use changes resulted in an increase in the annual runoff for the period of 1996–2005 at a rate of 12.4% and that for the period of 2006–2014 at a rate of 14.5%.

Table 6 shows the relative contributions of climate change and land use/cover change to the change in polder runoff. For the period of 1996–2005, the annual runoff increased by 79.7 mm, 101.4% of which was caused by climate change and −1.4% of which by land use/cover change. However, for the period 2006–2014, the annual runoff increased by 93.6 mm, −42.4% of which was induced by the climate change and 142.4% of which by land use/cover change. This result indicates that climate change was the primary driving force of the annual runoff change in the period of 1996–2005, whereas land use/cover change was the dominant reason for annual runoff change in the period of 2006–2014.

Table 6 | Relative effects of climate change and land use/cover change on average annual runoff

Period	Annual runoff/mm	ΔQ/mm	$\Delta Q_{climate}$/mm	ΔQ_{lucc}/mm	$I_{climate}$ (%)	I_{lucc} (%)
1986–1995	643.8					
1996–2005	723.5	79.7	80.8	−1.1	101.4	−1.4
2006–2014	737.4	93.6	−39.7	133.3	−42.4	142.4

Model performance and uncertainties

The model is relatively simple, flexible, and computationally efficient, hence it shortens computation time and saves computation resources when modeling complicated scenarios. More importantly, the model is capable of running with limited data. Therefore, the developed model can be conveniently used in other polders, especially in ungauged areas. The case study also demonstrates that the improved WALRUS model has potential for use in investigating the effects of climate and land use changes on Asian lowland polder systems with paddy fields and pumping stations.

This study has several limitations. First, several important soil moisture parameters including b, ϕ_{ae}, and θ_S are estimated empirically based on the results from Clapp & Hornberger (1978), which were obtained from laboratory experiments based on the 1,446 soil samples throughout the United States of America. Hence, the discrepancies in climatic zones, cropping plants, and human activities could induce some differences in these parameters between American agricultural areas and Asian agricultural zones for the same soil texture (soil type). Consequently, the estimated parameters might introduce uncertainties in the model results. Therefore, a table with appropriate values of the soil moisture parameter based on soil samples from Asian agricultural zones, such as South China and East China, should be established to improve the accuracy of the model results and to facilitate the application of the model in Asian agricultural polders. Second, the improved model requires further validation based on long-time series data and small time scales to obtain more robust results. Confined by the limited data, this study only employed 3 years' monthly data to test the model. As a matter of fact, this dataset is insufficient for model testing when the tested model is applied to quantify the relation between climate change and hydrological processes. This is also a common problem for most Chinese polders, where the hydrological observations mainly focus on short-term rainfall events or monthly time series thus far. Therefore, further works should collect long-term data on a daily basis by setting up fixed hydrological stations or recording the running time of pumping stations in the study area. However, even with these uncertainties, the current results still provide a good description of the hydrological processes in Asian agricultural polders considering the present conditions and the good agreement of the simulated runoff value with the observed value.

Water management implications of climate and land use/cover changes for the catchment

With respect to the effect of land use change alone, the shift from rice–wheat rotation to double-rice cropping and the expansion of the residential area intensified polder runoff, which could exacerbate flooding and sedimentation risks and block the irrigation ditch of a large agricultural polder, especially during the rainy season. Thus, this estimate may be applicable in the development of adaptation strategies, such as land use planning and agricultural water resources management.

The hydrological change of agricultural polder has the potential to affect water quality and the export of non-point source pollution. Combined with increased fertilization and population size in Poyang Lake basin (Wang *et al.* 2006; Gao & Jiang 2012; Ma *et al.* 2015), the increased annual water yield caused by the climate and land use/cover changes over the past decades likely resulted in high water nitrate and phosphorus concentrations within the catchment and contributed to the excessive nutrient and sediment exported to the adjoining river (Oenema & Roest 1998; Bonte & Zwolsman 2010; van der Velde *et al.* 2010). This result would ultimately degrade the water quality of the entire floodplain basin, and even probably induce the eutrophication of Poyang Lake. Therefore, the results of this study have implications for the management of water quality and aquatic ecosystem health in the floodplain basin.

CONCLUSIONS

In this study, an improved WALRUS model was applied to evaluate and discriminate the effects from observed historical climate change and land use/cover change on the seasonal and annual runoff of a Chinese agricultural polder in the past two decades (1996–2005 and 2006–2014) on the basis of available hydro-climatic data. The good agreement between the modeled and observed monthly runoff indicated that the model can provide a reasonable estimate of monthly polder runoff.

Climate change caused a significant increase in the runoff during the autumn–winter transition (November–January) and midsummer (August) months, and a slight decrease in the other months, especially in the early spring and autumn of the latter two periods. Land use/cover remained relatively constant during the period 1996–2005 compared to the baseline period. As a result, land use/cover change alone had less effect on the runoff during this period. However, following the implementation of China's agricultural policy reform since 2004 and advances in agricultural technology, the major land use/cover change during the period of 2006–2014 was primarily the shift from rice–wheat rotation to a dominant double-rice cropping system in the paddy field and the expansion of the residential area. This land use/cover change contributed to an increase in polder runoff throughout the year (except for April and September) by increasing the amount of irrigation water.

The estimates on the combination of both effects showed that the seasonal distribution of runoff was in accordance with distribution influenced by climate change separately for the period of 1996–2005. This result indicated that climate change was a primary driving force of the runoff change during this period. On the other hand, the runoff during the period of 2006–2014 was sensitive to both climate change and land use/cover change. The runoff in the autumn–winter transition and midsummer months had a higher increase than the runoff influenced by climate change or land use/cover change alone. However, the change trend was mitigated in the other months because the effect of climate change was opposite to that of land use/cover change. Moreover, the combined effect of climate and land use changes also changed the amount of annual runoff with an increase of 12.4% for the period of 1996–2005 and 14.5% for the period of 2006–2014, although the effect was lower than that on monthly runoff.

The discrimination between the different drivers of annual runoff indicated that climate change played a crucial role in the increased annual runoff for the period 1996–2005, while the contribution of land use/cover change to the increase in runoff was higher than the contribution of climate change during the period 2006–2014.

Despite the uncertainties of this study, the model results and approaches proposed might have some implications for flood control and water quality management, and may provide guidance in the design of adaptation strategies for dealing with environmental issues arising from climate and land use/cover changes. Further efforts will be oriented towards validating the model further by using long-term daily datasets and appropriate soil moisture parameter values for a specific study area from location-specific soil samples.

ACKNOWLEDGEMENTS

This study was financially supported by National Basic Research Program of China (No. 2012CB417006), Major Water Resources Science and Technology Program of Jiangxi Water Resources Department (KT201406), and 135″ Key Program in Nanjing Institute of Geography and Limnology, Chinese Academy of Sciences (NIGLAS2012135005). We acknowledge Dr Huang Jiacong for useful suggestions for the model modification and Claudia Brauer for providing the code of original lumped WALRUS model. We also wish to thank the anonymous reviewers and the editor for their valuable comments.

REFERENCES

Awan, U. K., Liaqat, U. W., Choi, M. & Ismaeel, A. 2016 A SWAT modeling approach to assess the impact of climate change on consumptive water use in Lower Chenab Canal area of Indus basin. *Hydrol. Res.* doi:10.2166/nh2016102.

Bonte, M. & Zwolsman, J. J. G. 2010 Climate change induced salinisation of artificial lakes in the Netherlands and consequences for drinking water production. *Water Res.* **44**, 4411–4424.

Bouwer, L. M., Bubeck, P. & Aerts, J. C. 2010 Changes in future flood risk due to climate and development in a Dutch polder area. *Global Environ. Change* **20**, 463–471.

Brauer, C., Torfs, P., Teuling, A. & Uijlenhoet, R. 2014a The Wageningen Lowland Runoff Simulator (WALRUS): application to the Hupsel Brook catchment and the Cabauw polder. *Hydrol. Earth Syst. Sci.* **18**, 4007–4028.

Brauer, C. C., Teuling, A. J., Torfs, P. & Uijlenhoet, R. 2014b The Wageningen Lowland Runoff Simulator (WALRUS): a

lumped rainfall–runoff model for catchments with shallow groundwater. *Geosci. Model Dev.* **7**, 2313–2332.

Cai, S., Shi, H., Xu, Y. Q., Cui, Y. L., Liu, F. P., Yang, W. X. & Xie, W. T. 2014 Research on the intensifying irrigation modes of double season rice in irrigation areas of Ganfu Plain. *China Rural Water Hydropower* **55**, 11–14.

Chen, Z. G. 1987 A tentative idea of the realignment and economic development of the dike area around Poyang Lake. *J. Jiangxi Normal Uni. (Nat. Sci.)* **11**, 122–128.

Cheng, W. H., Wang, C. H. & Zhu, Y. 2006 *Taihu Basin Model*. HoHai University Press, Nanjing.

Clapp, R. B. & Hornberger, G. M. 1978 Empirical equations for some soil hydraulic properties. *Water Resour. Res.* **14**, 601–604.

Estes, M. G., Al-Hamdan, M. Z., Ellis, J. T., Judd, C., Woodruff, D., Thom, R. M., Quattrochi, D., Watson, B., Rodriguez, H., Johnson, H. & Herder, T. 2015 A modeling system to assess land cover land use change effects on SAV habitat in the Mobile Bay estuary. *J. Am. Water. Resour. Assoc.* **51**, 513–536.

Folton, N., Andréassian, V. & Duperray, R. 2015 Hydrological impact of forest-fire from paired-catchment and rainfall–runoff modelling perspectives. *Hydrolog. Sci. J.* **60**, 7–8.

Gao, J. F. 2004 *Watershed Data Model and Distributed Hydrological Modeling*. University of Chinese Academy of Sciences, Nanjing, China.

Gao, J. F. & Jiang, Z. 2012 *Conservation and Development of China's Five Largest Freshwater Lakes*. Science Press, Beijing.

Guo, Y. Y. 1997 *Irrigation and Drainage Engineering*. China Water Power Press, Beijing.

Guo, J. T., Zhang, Z. Q., Wang, S. P., Peter, S. & Yao, A. K. 2014 Appling SWAT Model to explore the impact of changes in land use and climate on the streamflow in a watershed of Northern China. *Acta Eco. Sinica* **34**, 1559–1567.

Guse, B., Kail, J., Radinger, J., Schroder, M., Kiesel, J., Hering, D., Wolter, C. & Fohrer, N. 2015 Eco-hydrologic model cascades: simulating land use and climate change impacts on hydrology, hydraulics and habitats for fish and macroinvertebrates. *Sci. Total Environ.* **533**, 542–556.

Hargreaves, G. L. & Samani, Z. A. 1985 Reference crop evapotranspiration from temperature. *J. Irr. Drain. DIV-ASCE* **111**, 113–124.

Hellmann, F. & Vermaat, J. E. 2012 Impact of climate change on water management in Dutch peat polders. *Ecol. Model.* **240**, 74–83.

Immerzeel, W. W., Van Heerwaarden, C. C. & Droogers, P. 2009 Modelling climate change in a Dutch polder system using the FutureViewR modelling suite. *Comput. Geosci.* **35**, 446–458.

Jiang, J. H., Lai, X. J. & Huang, Q. 2007 The characteristics of flood responses to the restoration of polders on Dongting Lake, China. *Hydrolog. Sci. J.* **52**, 671–685.

Júnior, J. S., Tomasella, J. & Rodriguez, D. A. 2015 Impacts of future climatic and land cover changes on the hydrological regime of the Madeira River basin. *Clim. Change* **129**, 117–129.

Kendall, M. G. 1975 *Rank Correlation Methods*. Griffin, London, UK.

Kovar, P., Pelikan, M., Hermanovska, D. & Vrana, I. 2014 How to reach a compromise solution on technical and non-structural flood control measures. *Soil Water Res.* **9**, 143–152.

Legesse, D., Vallet-Coulomb, C. & Gasse, F. 2003 Hydrological response of a catchment to climate and land use changes in Tropical Africa: case study South Central Ethiopia. *J. Hydrol.* **275**, 67–85.

Li, Y. L., Zhang, Q., Yao, J., Werner, A. D. & Li, X. 2013 Hydrodynamic and hydrological modeling of the Poyang Lake catchment system in China. *J. Hydrol. Eng.* **19**, 607–616.

Li, W. Y., Jiang, L. G. & Li, P. 2014 The spatio-temporal pattern of rice cropping systems in the polder area of Poyang Lake during 2000–2010. *Resour. Sci.* **36**, 809–816.

Li, Y. L., Zhang, Q., Werner, A. & Yao, J. 2015 Investigating a complex lake-catchment-river system using artificial neural networks: Poyang Lake (China). *Hydrol. Res.* **46**, 912–928.

Luo, Y., Su, B., Zhang, Q. & Yang, W. 2013 Identifying and modeling confined hydrological processes in Plain Polders. *Resour. Sci.* **35**, 594–600.

Ma, G. W., Wang, S. R., Wang, Y. Y., Zuo, D. P., Yu, Y. & Xiang, B. 2015 Temporal and spatial distribution characteristic of nitrogen and phosphorus and diffuse source pollution load simulation of Poyang Lake Basin. *Acta Sci. Circumstantiae* **35**, 1285–1291.

Mann, H. B. 1945 Nonparametric tests against trend. *Econometrica* **13**, 245–259.

Mehdi, B., Ludwig, R. & Lehner, B. 2015 Evaluating the impacts of climate change and crop land use change on streamflow, nitrates and phosphorus: a modeling study in Bavaria. *J. Hydrol.* **4** (Part B), 60–90.

Neupane, R. P. & Kumar, S. 2015 Estimating the effects of potential climate and land use changes on hydrologic processes of a large agriculture dominated watershed. *J. Hydrol.* **529** (Part 1), 418–429.

Oenema, O. & Roest, C. W. J. 1998 Nitrogen and phosphorus losses from agriculture into surface waters; the effects of policies and measures in The Netherlands. *Water Sci. Technol.* **37**, 19–30.

Pavanelli, D. & Capra, A. 2014 Climate change and human impacts on hydroclimatic variability in the Reno River catchment, Northern Italy. *Clean (Weinh)* **42**, 535–545.

Sneyers, R. 1975 *Sur l'Analyse Statistique des Séries d'Observations*. Secrétariat de l'Organisation Météorologique Mondiale.

Su, B. L., Luo, Y. X., Chen, H. W., Wan, B. H. & Wang, T. 2013 Modeling of hydrological processes in lower plain polder of the Ganjiang River. *South-to-North Water Transfers Water Sci. Technol.* **11**, 39–43.

Syvitski, J. P., Kettner, A. J., Overeem, I., Hutton, E. W., Hannon, M. T., Brakenridge, G. R., Day, J., Vorosmarty, C., Saito, Y., Giosan, L. & Nicholls, R. J. 2009 Sinking deltas due to human activities. *Nat. Geosci.* **2**, 681–686.

Tian, P. 2012 *Impacts of Climate and Land Use Change on Streamflow: A Case Study in the Poyang Lake Basin*. Doctor, Northwest Agricultural and Forestry University, Yangling.

van der Velde, Y., Rozemeijer, J. C., de Rooij, G. H., van Geer, F. C. & Broers, H. P. 2010 Field-scale measurements for separation of catchment discharge into flow route contributions. *Vadose Zone J.* **9**, 25–35.

Wang, J. N., Yan, W. J. & Jia, X. D. 2006 Modeling the export of point sources of nutrients from the Yangtze River basin and discussing countermeasures. *Acta Sci. Circumstantiae* **26**, 658–666.

Xie, X. H. & Cui, Y. L. 2011 Development and test of SWAT for modeling hydrological processes in irrigation districts with paddy rice. *J. Hydrol.* **396**, 61–71.

Yan, R. H., Gao, J. F., Dong, C. Y. & Huang, J. C. 2015 Assessment of ecosystem services for polder terrestrial ecosystem in Taihu Basin. *Res. Environ. Sci.* **28**, 393–400.

Yan, R. H., Huang, J. C., Wang, Y., Gao, J. F. & Qi, L. Y. 2016a Modeling the combined impact of future climate and land use changes on streamflow of Xinjiang Basin, China. *Hydrol. Res.* **47**, 356–372.

Yan, R. H., Gao, J. F. & Huang, J.C. 2016b WALRUS-paddy model for simulating the hydrological processes of lowland polders with paddy fields and pumping stations. *Agr. Water Manage.* **169**, 148–161.

Zhao, G. J., Hörmann, G., Fohrer, N., Gao, J., Li, H. & Tian, P. 2010 Application of a simple raster-based hydrological model for streamflow prediction in a humid catchment with polder systems. *Water Resour. Manag.* **25**, 661–676.

First received 20 October 2015; accepted in revised form 23 February 2016. Available online 3 May 2016